Acta Cryst. (1951). **4**, 531

A New Approach to Crystal-Structure Analysis

By M. J. Buerger

Massachusetts Institute of Technology, Cambridge, Mass., U.S.A.

(*Received* 6 *April* 1951 *and in revised form* 25 *April* 1951)

In order to apply vector-set methods to the solution of Patterson syntheses, it is first pointed out that the Patterson synthesis is the vector set of the electron density provided that the Patterson function is defined as an integral and not as an average of the electron-density product. With this proviso, vector-set methods can be applied to solve the Patterson synthesis for the electron density. The most appropriate vector-set method is the synthesis of the vector-set points into n identical n-gons. To do this with Patterson syntheses, one sets up a function of the Patterson values at the vertices of an image polygon, called an *image-seeking function.* Such a function has the property of attaining a high value when the polygon is in image position, but zero when it is not. Two such functions have been proposed, a *product function* and a *minimum function.* The properties of these functions are discussed. These functions bear an inequality relation to the electron density, and the inequality is strengthened by combining functions to produce others of greater rank. Application of this theory leads to a map of the function which is essentially an approximate map of the electron density. The theory is illustrated by application to the solution of the structure of berthierite, $FeSb_2S_4$, from its Patterson projection. By combining maps of the minimum function for this crystal, one of rank 8 is readily attained which is sufficiently close to the electron density so that seven atoms in the asymmetrical unit are clearly distinguished. These have peaks of relative ranks 4 : 2 : 1, which is approximately the relative electron counts of Sb, Fe and S, respectively.

The relation between these methods and those of Clastre & Gay, Garrido, Robertson, and McLachlan, is briefly discussed. The methods of these authors are the equivalents of image methods as applied to sets of discrete points, although a different language is used to describe them. They have not advanced beyond methods for decomposing vector sets of discrete points, and cannot be expected to solve typical Patterson syntheses.

Introduction

For many years the opinion was held that the direct solution of crystal structures by X-ray means was, in general, impossible because, although the amplitudes of the diffracted waves could be experimentally determined, their phases could not. While carrying out some crystal-structure studies during the early part of the recent war, the writer realized that the impossibility of determining phases experimentally did not necessarily imply the impossibility of determining crystal structures. At the Lake George meeting of the American Society for X-ray and Electron Diffraction in June 1946, it was shown that there was a very simple relation between the electron-density map and the Harker synthesis (Buerger, 1946). After a brief excursion into the prediction of phases through the implication relation and aided by the 'squared crystal' concept (Buerger, 1948*a*, *b*), the writer's interest was turned to the corresponding problem in crystal space rather than in Fourier space. In this study it immediately became obvious that the Patterson synthesis could be solved.

An early attempt to relate the Patterson map to the electron-density map had been made by Wrinch (1939). She simplified the problem by considering a set of discrete points and its Patterson representation, which may be called the *vector set.* A major contribution was the introduction of the notion of an *image.* Wrinch showed that one can find in the vector set the several images of a point, a line, or even a triangle, these comprising sets of one, two or three points which occur in the original set of points. She also discussed the analysis of a vector set for the original set of points, but did not present a technique for performing an analysis in a general case.

Building on Wrinch's fundamental work, the writer developed several general methods for completely analyzing a vector set of points. These methods were first presented in a series of lectures on vector methods (Faculty of Philosophy, University of Rio de Janeiro, December 1948), and as a contribution entitled 'The status of crystal-structure analysis' which formed part of a symposium on the Results of Crystal Structure Studies (Pittsburgh Meeting of the American Crystallographic Society, June 1949); they appeared in print in March 1950 (Buerger, 1950*a*).* The general method was immediately extended so that it could be applied to the transformation of true Patterson syntheses to electron-density maps (Buerger, 1950*b*, *d*).

In order to apply vector-set methods to situations arising in actual crystal-structure analysis, two developments were needed. It does not necessarily follow

---

* The notation and theory of this 'Vector Set paper' are frequently referred to in the following discussion. For brevity it is designated by the symbol VS.

that because a vector set of discrete points can be solved, the Patterson synthesis of a crystal can be handled by the same methods. It is necessary to demonstrate the connection between a set of discrete points with its vector set, on the one hand, and the continuously variable electron density of a crystal, with its continuously variable Patterson representation, on the other. In the second place it is necessary to find a mechanism for finding images in the Patterson synthesis.

Extension of vector-set theory to continuously variable electron densities

It has been shown (Buerger, 1950*b*, *d*) that the vector set of a continuously variable electron density is indeed the Patterson synthesis, provided that the Patterson synthesis is defined in a particular way. In the original derivation of his function (Patterson, 1934, 1935), Patterson chose the average value of the electron-density product separated by a vector having components xyz, as the vector ranged over the cell. To emphasize this averaging characteristic, Patterson designated his function $A(xyz)$. If one starts with an electron density represented by the Fourier series

$$\rho(xyz)=\frac{1}{V}\sum_h\sum_k\sum_l Fe^{-2\pi i(hx+ky+lz)}, \tag{1}$$

then Patterson's averaging function comes out to have a Fourier representation

$$A(xyz)=\frac{1}{V^2}\sum_h\sum_k\sum_l F^2 e^{-2\pi i(hx+ky+lz)}. \tag{2}$$

On the other hand, the vector set of (1) turns out to be simply the integral of the electron-density product over the cell volume. The Fourier representation of this, which will be designated $P(xyz)$ to distinguish it from Patterson's original average, is

$$P(xyz)=\frac{1}{V}\sum_h\sum_k\sum_l F^2 e^{-2\pi i(hx+ky+lz)}. \tag{3}$$

Note that this synthesis is exactly the same as the Fourier representation of the electron density except that F^2's are substituted for F's. It is therefore identical with the writer's 'squared crystal' (Buerger, 1948*b*). The relation between the vector set of the electron density and the original Patterson averaging function is simply

$$P(xyz)=\frac{1}{V}A(xyz). \tag{4}$$

Scheme for analyzing Patterson syntheses suitable to automatic application

Having shown that the Patterson synthesis is essentially the vector set of the electron density, it becomes possible to analyze Patterson syntheses by vector-set methods. This implies that one hopes to find suitable functions which will automatically find images in a Patterson synthesis. The details of setting up such functions are reserved for a subsequent section.

The two general methods of solving a vector set are to synthesize its points into either a 'spectrum of polygons' (VS, p. 90) or into a set of n identical n-gons (VS, p. 92). The latter method is easily adapted to the solution of Patterson syntheses, and is particularly suited to the derivation of a quantitative relation between electron density and Patterson synthesis in the form of an inequality which increases in power as the n-gon is synthesized in successive stages from a '2-gon' (a line) to an n-gon.

In VS (p. 89) it was pointed out that a 'vector set can be synthesized into images of the primitive set in each of its points'. This is illustrated analytically by expressing the vector-set matrix as images of the n-gon:

$$\begin{matrix} aa & ab & ac & ad & ae \\ ba & bb & bc & bd & be \\ ca & cb & cc & cd & ce \\ da & db & dc & dd & de \\ ea & eb & ec & ed & ee \end{matrix} = \left.\begin{matrix} a(a+b+c+d+e) \\ b(a+b+c+d+e) \\ c(a+b+c+d+e) \\ d(a+b+c+d+e) \\ e(a+b+c+d+e) \end{matrix}\right\}, \tag{5}$$

$$= \left.\begin{matrix} -(a+b+c+d+e)\,a \\ -(a+b+c+d+e)\,b \\ -(a+b+c+d+e)\,c \\ -(a+b+c+d+e)\,d \\ -(a+b+c+d+e)\,e \end{matrix}\right\}. \tag{6}$$

The right side of (5) can be described as the image of the n-gon $(a+b+c+d+e)$ as seen from its separate points a, b, c, d and e. The rearrangement given in (6) follows by virtue of relation (4) of VS. The right side of (6) can be described as the image of the separate points a, b, c, d and e, as seen from the inverse polygon, the inverse character being required by the negative sign. These relations can be given very simple geometrical illustrations, shown in Figs. 1 and 2. In Fig. 1 is shown the points of a vector set assembled ('synthesized') into a set of nn-gons (n being 5 in the illustration). In order to put the discussion in somewhat more usual language than that used in VS, let each of the terms in the vector set on the left of (5) represent a vector. Then the right side of (5) can be interpreted to mean that these vectors can be gathered into sheafs of vectors. If some arbitrary point in the polygon is taken as representing the position of the polygon, then each sheaf of vectors can be represented by a single vector to this arbitrary point. Thus, instead of all the vectors from the origin to each point of the vector set, one can bulk together sets of points to form polygons, and substitute for each sheaf of vectors to the vertices of a polygon, a single vector from the origin to the representative point. This set of vectors is represented in Fig. 1. Fig. 2 illustrates that this same set of vectors determines a set of points which is the inverse polygon. This corresponds to the right of (6).

To see how this relation permits the solution of a vector set, assume, first, that the solution of the vector set is known. This means that in Fig. 1 the arrangement of points constituting one polygon is known. If this

n-gon is permitted to rove over the vector set, it encounters n positions where its points register with the points of the vector set. These positions are indicated by the crosses of Figs. 1 and 2. The set of such positions constitutes the inverse solution, and, furthermore, the vector matrix (6) shows that if the weighting of the images of the vector set is taken into account (Buerger, 1950*b*, *d*), the weighting of the points determined by the process, Fig. 2, also gives a correctly weighted solution of the vector set.

In this discussion it appears merely that if one knows the solution of the vector set and uses it in the above process, the solution is fed back in the form of the inverse solution. Actually the full solution has been assumed in the above discussion only for the purpose of illustrating the nature of the process. The process is much more powerful than this; for, if any minimum fragment of the solution is known, the entire solution can be found by the same means. That this is so can be demonstrated analytically by writing down, in matrix form, the process of solving a vector set by the procedure of synthesizing its points into a set of 2-gons, 3-gons, 4-gons and eventually n-gons. This stepwise synthesis is as follows:

$$\begin{array}{ccccc} aa & ab & ac & ad & ae\\ ba & bb & bc & bd & be\\ ca & cb & cc & cd & ce\\ da & db & dc & dd & de\\ ea & eb & ec & ed & ee \end{array} = \begin{array}{cccc} aa & ab & ac & a(d+e)\\ ba & bb & bc & b(d+e)\\ ca & cb & cc & c(d+e)\\ da & db & dc & d(d+e)\\ ea & eb & ec & e(d+e) \end{array}$$

$$= \begin{array}{ccc} aa & ab & a(c+d+e)\\ ba & bb & b(c+d+e)\\ ca & cb & c(c+d+e)\\ da & db & d(c+d+e)\\ ea & eb & e(c+d+e) \end{array}$$

$$= \begin{array}{cc} aa & a(b+c+d+e)\\ ba & b(b+d+c+e)\\ bc & c(b+d+c+e)\\ bd & d(b+c+d+e)\\ be & e(b+c+d+e) \end{array}$$

$$= \begin{array}{c} a(a+b+c+d+e)\\ b(a+b+c+d+e)\\ c(a+b+c+d+e)\\ d(a+b+c+d+e)\\ e(a+b+c+d+e) \end{array} \qquad (7)$$

This is merely a compact review of (9), (14), (15) and (16) of VS. It is the analytical representation of the process of collecting points of the vector set first into a set of line images, then adding a point to each line image to change them into triangle images, then adding a point to each triangle image to change them into quadrilateral images, then adding a point to each quadrilateral image to change them into pentagon images. For a fundamental set with $n=5$ points, this exhausts the points of the vector set, i.e. every point of the vector set is a member of one of the five pentagon images, each of which constitutes a solution. But for each stage in the process, a relation similar to (5), and therefore (6), is true. In other words, if any kind of image with $n \geqslant 2$ can be found in the vector set, the complete set of such images can be found. If the location in each such image of the set is spotted by means of a point associated with the image and having the weighting of that image, then the set of such points is the correctly weighted inverse solution. A graphical illustration of this is given in Figs. 3 and 4.

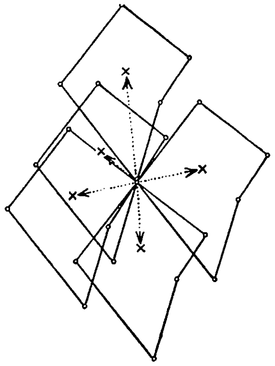

Fig. 1.

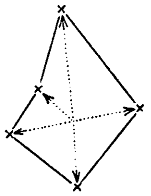

Fig. 2.

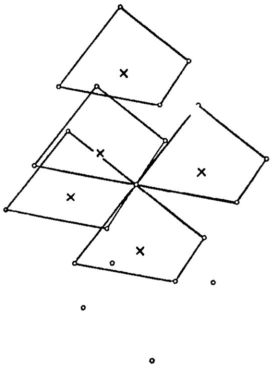

Fig. 3.

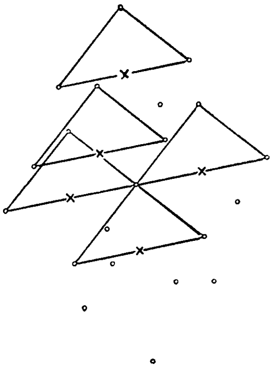

Fig. 4.

It should be observed that, if a line image is established and the line moved over the vector set parallel to itself, it might encounter two points fortuitously related so that they determine an equal and parallel line segment. If this accidental situation should arise, then the above procedure would lay down a false location of a line image owing to a purely fortuitous relation between a pair of points in the vector set. Such a registry of an image with a few accidentally related points of the vector set becomes the less probable the larger the number of points in the image with which registry must be simultaneously achieved. Thus, the success of the process described becomes the more certain as the value of p of the p-gon image becomes greater, attaining a maximum at $p=n$. This permits one to increase the certainty of a correct solution by exploring for the solution in stages. Thus, one would first select any point, connect it with the origin and thus establish a line. The images of this line can be found, and their weighted locations establish a tentative solution. If, for the reason mentioned above, or for reasons still to be discussed, there result too many points in the solution to conform to the n points of the fundamental set, the number of points in the tentative solution can be reduced by selecting one and then testing it by adding it to the original line in the solution. This constitutes a triangle, whose n images must occur in the vector set if the triangle is truly a part of the solution. If so, the new polygon (improved from a line with $p=2$ to a triangle with $p=3$) can be used to rove over the vector set. This three-point polygon is less likely to encounter locations of fortuitous registry with the points of the vector set than the line. But if there are still too many positions of registry, i.e. if the solution contains more than the n points of the fundamental set, then a point of the solution can be selected to add to the triangle to transform it into a quadrilateral, which can be used to explore the vector set for registry. Proceeding in this stepwise manner, a tentative solution established by line images can be pyramided to a solution certified by (*a*) exhausting the n^2 points of the vector set, and (*b*) by finding n locations of an n-gon which (*c*) themselves have the arrangement of the correctly weighted inverse n-gon.

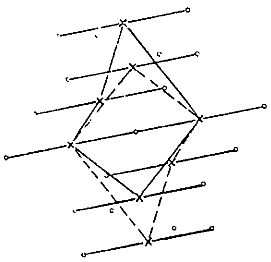

Fig. 5.

At this point it is desirable again to call attention (VS, p. 92) to the fact that it is impossible to distinguish between right-handed and left-handed line images. If, therefore, the fundamental set is noncentrosymmetrical, the first exploration for a solution with line images yields both a right-handed and a left-handed solution which are intermixed (Fig. 5) (Buerger, 1950*b*). These are joined by the line whose images in the vector set have been used for the solution. To rid the tentative solution of one of the unwanted enantiomorphous solutions, one need merely add any point of the tentative solution to the original line images, thus transforming them into triangle images (Fig. 4). In this general case, such triangle images are either left-handed triangles or right-handed triangles, depending on the choice of the added point. As this triangle roves the vector set, only one solution is found to be in registry. In this way an unwanted enantiomorphous solution can be eliminated (Buerger, 1950*c*, *d*).

The whole matter of enantiomorphous solutions can be avoided if the fundamental set is centrosymmetrical, provided one chooses as the original line for image-seeking a line from the origin to a vector point representing an 'interaction' between centrosymmetrically situated points in the fundamental set. Actually, this is a special aspect of the multiple-image situation, which is about to be discussed.

Multiplicity of Patterson peaks

To make a successful choice of line for an initial image requires a knowledge of the relative weights of the Patterson peaks. Patterson peaks may have multiple weight fortuitously, owing to the chance coincidence of two or more peaks, or this superposition may occur with exactness due to symmetry. The multiplicity due to symmetry is discussed in implication theory (Buerger, 1946). As a brief comment it may be noted that all inversion peaks (those due to the 'interaction' of two atoms which are equivalent by inversion) are single peaks, that reflection peaks (those due to the 'interaction' of two atoms which are equivalent by any reflection symmetry) are single when the plane is parallel to an odd-fold axis but double when parallel to an even-fold axis, whereas rotation peaks (those due to the 'interaction' of two atoms which are equivalent by rotation symmetry) are single for certain rotation operations, multiple for others.

The multiplicity of a Patterson peak can thus be judged by symmetry. It can also be judged by comparison with the origin peak. This origin peak has a volume $\sum_j Z_j^2$, where Z_j is the number of electrons in the jth atom and the summation is taken over the crystal cell. Since this volume is known, the volume of any peak on the Patterson synthesis can be calibrated in terms of it. Obviously, if a particular peak has a volume Z_j^2, it is a single symmetrical interaction, whereas if it has a volume of $2Z_j^2$, it is a double symmetrical interaction, etc.

Solutions resulting from multiple images

The penalty for choosing a multiple peak for forming a line to be used as a first image is to incur a multiple solution (Buerger, 1950*b*). That this is so is evident by making two points of the vector-set matrix the same point. Suppose that in the fundamental set there are two pairs of points so arranged that the vector relating the points of one pair is the same as the vector relating the points of the other. The two vectors coincide in vector space, and the point at the end of the vectors is a multiple point. The line connecting this point with the origin has two sets of images. One is the set of images of one of the parallel lines in the fundamental set, the other is the set of images of the other line in the fundamental set.

The formal treatment of this is as follows. Let the points of the crystal set be $a+b+c+d+e$, and suppose that the vector $\overrightarrow{bc}=\overrightarrow{de}$. Then the points bc and de coincide in the vector set so

$$bc=de. \tag{8}$$

If the origin point is added to both sides of this equality, there results

$$bb+bc=dd+de. \tag{9}$$

Expressed in the form of line images, this is equivalent to

$$b(b+c)=d(d+e). \tag{10}$$

This means that the image of the line $(b+c)$ is the same if seen from b as the image of the line $(d+e)$ if seen from d. In other words, these line images coincide. But, according to the image interpretation of the vector-set matrix, each such line also has its column of images, i.e. all the lines blocked out in the following matrix are parallel but distinct, except the two which are identical according to (10). These are tied together:

$$\left.\begin{array}{ccc} aa & \boxed{ab \quad ac} & \boxed{ad \quad ae} \\ ba & \boxed{bb \quad bc} & \boxed{bd \quad be} \\ ca & \boxed{cb \quad cc} & \boxed{cd \quad ce} \\ da & \boxed{db \quad dc} & \boxed{dd \quad de} \\ ea & \boxed{eb \quad ec} & \boxed{ed \quad dd} \end{array}\right\}. \tag{11}$$

This decomposition shows that if one should select the line $bb+bc$, i.e. $b(b+c)$, as the initial line image, more than one column of images would be found to be the apparent set of images. But this does not exhaust the total number of lines found, for the lower left-hand pair of points, $da+ea$, is centrosymmetrical with the upper right-hand pair, $ad+ae$, and consequently represents a parallel line. The total number of lines found is better demonstrated by synthesizing the points of the matrix into a certain set of line images and their centrosymmetrical equivalents. If there are *no* coincident vectors, the number of parallel, equal lines for a fundamental set of $n=5$ is four, plus four more centrosymmetrically related lines:

$$\left.\begin{array}{cccc} aa & ab & ac & \boxed{ad \quad ae} \\ ba & bb & bc & \boxed{bd \quad be} \\ ca & cb & cc & \boxed{cd \quad ce} \\ \boxed{\begin{array}{c} da \\ ca \end{array}} & \boxed{\begin{array}{c} db \\ cb \end{array}} & \boxed{\begin{array}{c} dc \\ cc \end{array}} & \begin{array}{cc} \boxed{dd \quad de} \\ cd \quad ce \end{array} \end{array}\right\}. \tag{12}$$

But if degeneracy (8) with its concomitant (9) and (10) occur, then the following *ten* lines are equal, parallel and apparent images:

$$\left.\begin{array}{cccc} aa & \boxed{ab \quad ac} & & \boxed{ad \quad ae} \\ \boxed{\begin{array}{c} ba \\ ca \end{array}} & \boxed{\begin{array}{c} bb \\ cb \end{array}} & \boxed{bc} \quad cc & \begin{array}{c} \boxed{bd \quad be} \\ \boxed{cd \quad ce} \end{array} \\ \boxed{\begin{array}{c} da \\ ea \end{array}} & \boxed{\begin{array}{c} db \\ eb \end{array}} & \boxed{\begin{array}{c} dc \\ ec \end{array}} & \begin{array}{cc} \boxed{dd \quad de} \\ \boxed{ed} \quad ee \end{array} \end{array}\right\}. \tag{13}$$

These relations for vector sets based upon fundamental sets without and with parallel vectors are illustrated in Fig. 6.

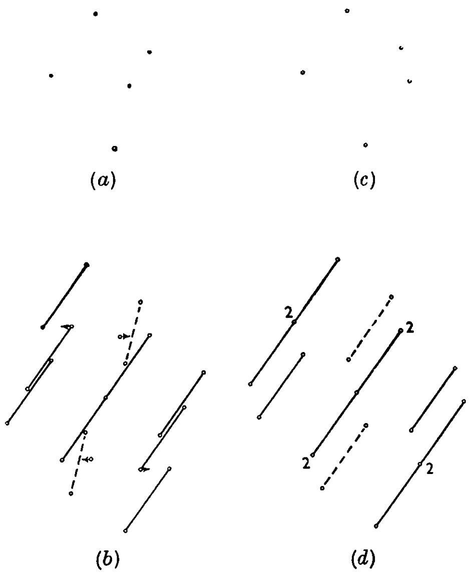

Fig. 6. The consequences of decomposing a vector set by using a multiple line-image. (*a*) A fundamental 5-point set without parallel vectors. (*b*) The vector set of Fig. 6 (*a*). The full lines are the eight true images of a line. (*c*) The fundamental set of Fig. 6 (*a*) altered by shifting one of the five points so that the set contains equal, parallel vectors. (*d*) The vector set of Fig. 6 (*c*). The full lines correspond to the line images shown in full lines in Fig. 6 (*b*). The broken lines, which were distinct in Fig. 6 (*b*), now form part of a set of eight parallel and equal lines, the additional lines arising from the multiple nature of the vector point used to form the initial line image. The double weighting of points arises from the migration of points of Fig. 6 (*b*) in the directions of the arrows.

In solving a vector set or Patterson synthesis, one is faced with the selection of the appropriate peak for beginning the decomposition. A common example of the situation is illustrated in Fig. 7, which represents a simple centrosymmetrical fundamental set. Note that the points related by the inversion determine a vector, shown as a full line, which is, in general, parallel to no other vector. In the vector set (Fig. 7 (*b*)) this 'interaction' is single. If this single point is connected with the origin, and the images of the resulting line are used to decompose the vector set, a single solution (Fig. 7 (*c*)) results. On the other hand, 'interactions' between points not related by the inversion in Fig. 7 (*a*) (in other words, unsymmetrical 'interactions') determine a double point in the vector set (Fig. 7 (*b*)). If such a point is connected with the origin and the images of the resulting line are used to decompose the vector set, a pair of intermixed solutions results. These necessarily have the original line in common. These two solutions are translated equivalents. Since a translation combined with an inversion is another inversion located at half the translation from the first inversion, it follows that such a double solution contains the true inversion center of the solution plus a false center which relates the two solutions. A similar symmetrical duplication of solutions occurs with other symmetry elements.

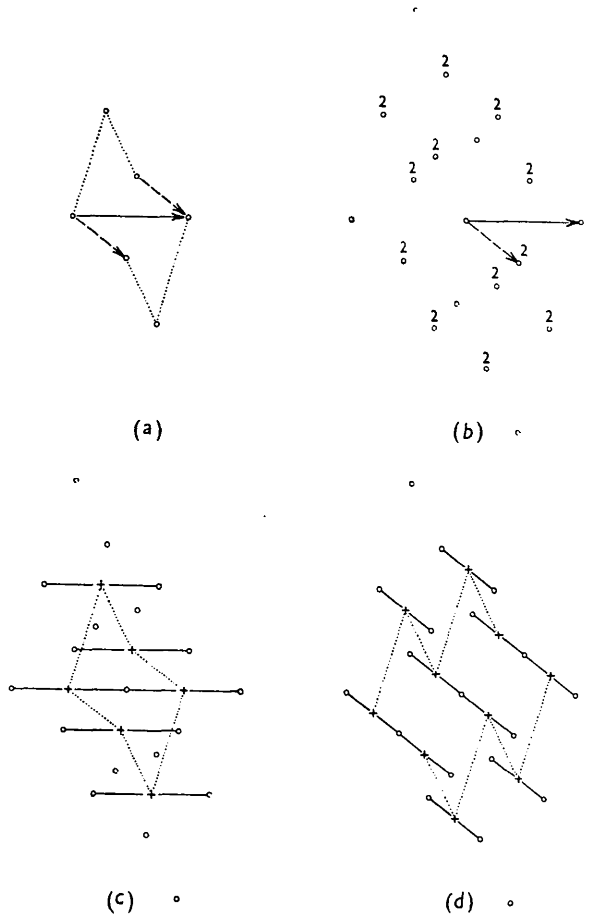

Fig. 7.

Image-seeking functions

One can apply the theory just discussed in one of two ways. The rather obvious way is to attempt to locate peaks in the Patterson synthesis and then find images defined by them by some graphical method. Such a scheme is difficult of application because many Patterson peaks are ordinarily swamped by background and hence not distinguishable. Furthermore, regions of high value of the Patterson function are frequently collections of unresolved peaks. The practicability of using such methods is increased by transforming the original Patterson synthesis into a 'sharpened Patterson' synthesis (Patterson, 1935; Buerger, 1950*b*), or a 'focused' synthesis (Buerger, 1950*c*). The effect of this transformation is to provide greater resolution of the n^2 peaks in the Patterson cell.

An alternative and preferred method is to set up a function which will automatically perform the job of finding the locations of images in the Patterson synthesis. Such a function is appropriately called an *image-seeking function.* To appreciate the desired characteristics of such a function, return to Fig. 1, and suppose that the solution is known, i.e. that one knows the relative positions of the vertices of one solution polygon. These relative positions can be defined by the origin plus $(n-1)$ other points, specifically 000, $u_1v_1w_1$, $u_2v_2w_2$, $u_3v_3w_3$, $u_4v_4w_4$ in this case. Let this polygon be moved to another location of the cell by a translation whose components are xyz. In the new location the co-ordinates of the vertices are

$$\left.\begin{array}{l} 0\ 0\ 0+xyz \\ u_1v_1w_1+xyz \\ u_2v_2w_2+xyz \\ u_3v_3w_3+xyz \\ u_4v_4w_4+xyz \end{array}\right\} \qquad (14)$$

First suppose, for clearness, that the Patterson synthesis has the simple form of a vector set of discrete weighted points which do not coincide with one another. A desirable image-seeking function would be some function of the Patterson synthesis at the co-ordinates given in (14) such that the function would have a value of zero when the translation xyz does not cause the original polygon to coincide with one of its images, but which would have a high value when the translation xyz does cause coincidence to occur.

The product function

Two rather obvious functions of this nature have been suggested and tried. One kind may be termed a *product function* (Buerger, 1950*b*, *d*). This is simply the product of the values of the Patterson function at the p vertices of the image-seeking polygon. As the polygon (pentagon in Fig. 1) is allowed to rove over the volume of the Patterson cell, x, y and z of (14) assume all values. The product

$$\begin{aligned} \Pi_5(xyz) = {} & P(000+xyz) \\ & \times P(u_1v_1w_1+xyz) \\ & \times P(u_2v_2w_2+xyz) \\ & \times P(u_3v_3w_3+xyz) \\ & \times P(u_4v_4w_4+xyz) \qquad (15) \end{aligned}$$

has zero value for any xyz unless all five points coincide with a pentagon image of Fig. 1. When coincidence does occur (with appropriate values of xyz) then the product has a high value, and this is specifically related to the electron density $\rho(xyz)$ through the weighting of the image (Buerger, 1950*d*).

One does not ordinarily know the full solution when starting to interpret a Patterson synthesis. Usually one can only recognize a point, say at $u_1v_1w_1$, as having single weight, and one wishes to construct a function which seeks an image of the line formed by connecting this point and the origin (Fig. 8 (*a*)). The partial product composed of the first two terms of (15), namely,

$$\begin{aligned}\Pi_2(xyz) = {} & P(000+xyz) \\ & \times P(u_1v_1w_1+xyz), \qquad (16)\end{aligned}$$

seeks and finds the images of this line, since it has zero value whenever the translation xyz does not superpose the original line on one of its images. Except for the original line from 000 to $u_1v_1w_1$, all such non-zero products are related to the electron density at the corresponding point in the fundamental set by the simple relation (Buerger, 1950*d*)

$$\rho(xyz) = \frac{1}{P(u_1v_1w_1)} \sqrt{\Pi_2(xyz)}. \qquad (17)$$

In case overlap of Patterson peaks does occur, as it usually does in the Patterson synthesis of a real crystal, the value of one or more terms in Π is fortuitously increased; consequently the right of (17) is increased. But the inequality

$$\rho(xyz) \leqslant \frac{1}{P(u_1v_1w_1)} \sqrt{\Pi_2(xyz)} \qquad (18)$$

still is valid.

This relation is readily generalized. If an image-seeking product-function is constructed of p terms for the purpose of seeking images of p-gons (Fig. 9), the relation between the electron density and the product function is

$$\rho(xyz) \leqslant \frac{1}{P(u_1v_1w_1) \times P(u_2v_2w_2) \times \ldots \times P(u_pv_pw_p)} \times p\,\sqrt{\Pi_p(xyz)}. \qquad (19)$$

When any image found by (19) includes the origin as one of its vertices, the inequality is somewhat less powerful, since one of the terms in $\Pi_p(xyz)$ is the weight of the origin peak. But these very images merely feed back information which has been put into the original image-seeking function, so that no real loss of information occurs owing to this circumstance.

The writer,* and subsequently Patterson,† have made actual use of the Π_2 function in solving two-dimensional Patterson maps of crystals whose structures had previously been unknown. The results of applying the Π function appear to be good in instances where the structure of the crystal is somewhat open, and also when used with crystals having a few heavy atoms embedded in a structure of lighter ones. The product function has certain disadvantageous features, and also it is more difficult to derive than the minimum function, a discussion of which follows in the next section.

When a tentative solution is achieved by (18), the strength of the inequality can be improved by adding to the 2-gon image used in forming function (16), one or more new points suggested by the solution. Having started the solution with function (16), one is then able to use function (15). This provides the more powerful inequality (19). In other words, the electron density of the crystal can be approached by successive approximations. This general process is further discussed in the next section.

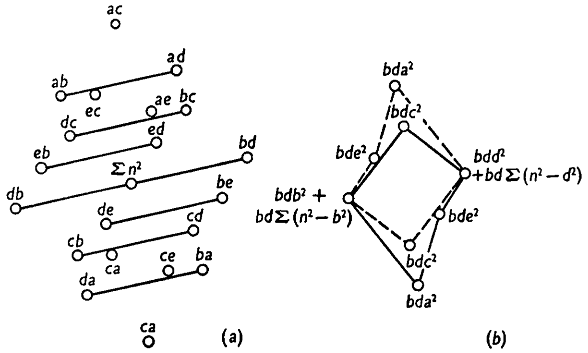

Fig. 8.

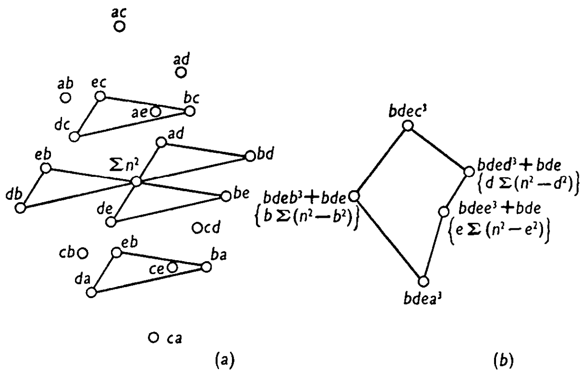

Fig. 9.

The minimum function

An unfortunate feature of the product function is caused by the continuous background of the Patterson synthesis. As the polygon roves this synthesis, the product function has a background value when all vertices of the polygon are on background. But when one or more of its vertices make chance registry with Patterson peaks, the function has a higher-than-background value. Such chance coincidences, therefore, produce small false peaks in the map of the product function which do not correspond to any feature on the electron-density maps.

A more desirable kind of function would be one which had a continuously low value so long as even one vertex of the polygon was on background, since such a circumstance corresponds with *not* finding an image

---

* Demonstrated as part of a lecture on the interpretation of the Patterson synthesis given to the North American Philips Diffraction School, 6 October 1950.

† Informally presented as part of a discussion of a paper given at the Washington meeting of the American Crystallographic Association, 15 February 1951.

of the polygon. The writer has devised the *minimum function* (Buerger, 1950*e*) for this purpose. The minimum function is defined as the minimum value of the several Patterson values (weighted, if necessary) which occur at the vertices of the polygon used to search for images of itself. Let the original polygon have p vertices at 000, $u_1v_1w_1$, $u_2v_2w_2, \ldots, u_pv_pw_p$. When the polygon is translated by xyz, its vertices have p sets of co-ordinates similar to those listed in (14). The minimum value, designated by the symbol M, may then be represented by

$$\begin{aligned} M_p(xyz) = M\{&P(000+xyz); \\ &K_1P(u_1v_1w_1+xyz); \\ &K_2P(u_2v_2w_2+xyz); \\ &K_{p-1}P(u_{p-1}v_{p-1}w_{p-1}+xyz)\}, \end{aligned} \tag{20}$$

where the K's are constants which normalize the relative values of the Patterson function at the several vertices of the polygon to the same value. The reason for this normalization is as follows: The exact registry of a polygon with an image location depends equally on the registry of each vertex, regardless of the value of the Patterson function at that vertex. To assure equal representation of each point in the operation of the minimum function, the Patterson values at the several points are scaled to normalize them to the same value. For example, if the polygon is $a+b+c+d+e$, the Patterson values at the vertices are proportional to a, b, c, d and e, respectively. They can all be normalized to a (for example) by multiplying the Patterson 'weight' at b by $a/b=K_1$, at c by $a/c=K_2$, etc. The polygon has now been transformed into one in which all vertices have the same weight.

A simple and convenient application of the minimum function is to images composed of centrosymmetrical 'interactions', i.e. 'interactions' between atoms which are centrosymmetrically situated in the crystal structure. The relation between the electron density and M_2 is very simply demonstrated by reference to Fig. 10. Fig. 10 (*a*) shows a simple centrosymmetrical fundamental set, while Fig. 10 (*b*) shows its Patterson function. Note that all centrosymmetrical 'interactions', namely, *aa*, *bb* and *cc*, have single weight, whereas all others are multiple. If a line from the origin to *aa* is established as a line whose images are to be found, one notes that the minimum values at the ends of the line when in image position have the very simple form

$$^aM_2(xyz) = 2\rho_a\rho(xyz). \tag{21}$$

The only exception to this occurs for the images containing the origin, for which the coefficient 2 in (21) does not appear owing to the unit nature of point *aa*. Since such images merely feed back information put into the formation of the minimum function, no real loss of information is incurred by this exception.

Alternatively, the image *bb* could be connected with the origin to form a line, and the images of this line could be sought. Fig. 10 (*c*) shows that the minimum values at the ends of the line are related to the electron density by

$$^bM_2(xyz) = 2\rho_b\rho(xyz). \tag{22}$$

If the vector set is the Patterson synthesis of a real crystal, then, in general, overlaps of 'squared atoms' (Buerger, 1948*b*) occur in the Patterson synthesis. In such instances (21) and (22) have enhanced values on their left-hand sides, so that they become inequalities of the same general form. The information from two such inequalities can be combined to give a more powerful inequality, thus:

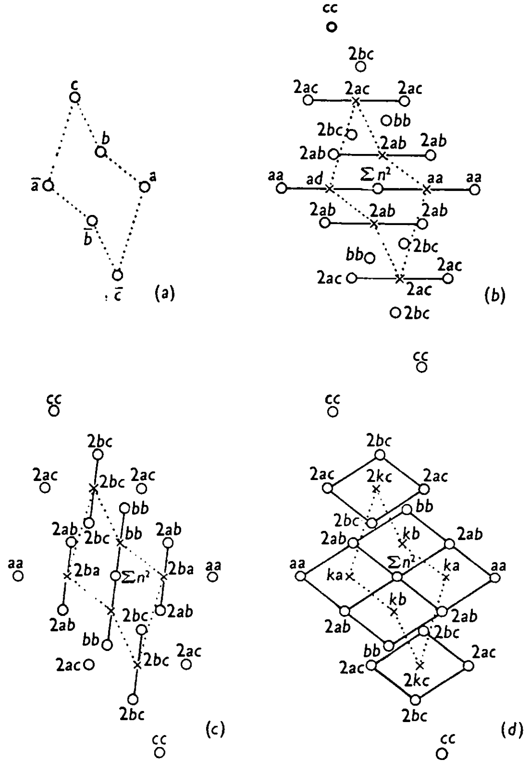

Fig. 10.

$$\frac{1}{2\rho_a}\,{}^aM_2(xyz) \geqslant \rho(xyz), \tag{23}$$

$$\frac{1}{2\rho_b}\,{}^bM_2(xyz) \geqslant \rho(xyz), \tag{24}$$

$$M\left\{\frac{1}{2\rho_a}\,{}^aM_2(xyz);\quad \frac{1}{2\rho_b}\,{}^bM_2(xyz)\right\} \geqslant \rho(xyz). \tag{25}$$

The reason why (25) is more powerful than either (23) or (24) is that the left-hand member of (23) may have a lower value at $x_1y_1z_1$ and the left-hand member of (24) may have a lower value at $x_2y_2z_2$. Since (25) combines the minimums of both relations, its left-hand member has the lower value at both $x_1y_1z_1$ and $x_2y_2z_2$.

The graphical representation of (23) is given in Fig. 10 (*b*), that of (24) in Fig. 10 (*c*). The combination of (23) and (24), namely, (25), is represented in Fig. 10 (*d*). This shows that the combination of two minimum functions which each seek line images is equivalent to a minimum function which seeks quadrilateral images. As a generalization of this combinatorial relation, it can be stated that the minimum of two appropriately weighted minimum functions is a new valid minimum function of higher rank and greater power. Thus, (23), (24) and (25) illustrate the combinatorial relation

$$M\left\{\frac{1}{2\rho_a}\,{}^{a}M_2(xyz);\quad \frac{1}{2\rho_b}\,{}^{b}M_2(xyz)\right\}={}^{ab}M_4(xyz), \tag{26}$$

and (25) shows that

$${}^{ab}M_4(xyz)\geqslant\rho(xyz). \tag{27}$$

A more general statement of the combinatorial properties of minimum functions can be expressed as follows:

$$M\{C_pM_p(xyz);\; C_qM_q(xyz)\}=M_{p+q}(xyz), \tag{28}$$

where the C's are constants concerned with the weighting of the images used in forming the original minimum functions. Relation (28) corresponds with adding a p-gon image to a q-gon image to form a $(p+q)$-gon image, as discussed in an earlier section of this paper.

Relation (26) is of great practical utility. It implies that the decomposition of a Patterson map by one line image can be combined with the decomposition by a second line image to form a close approximation to the electron density (27). If the two Patterson peaks, aa and ab, used to establish the line images are the centrosymmetrical 'interactions' of the same species of atom, then $\rho_a=\rho_b$, and the relation degenerates to the simple form

$$M\{{}^{a}M_2(xyz);\; {}^{b}M_2(xyz)\}=2\,{}^{ab}M_4(xyz). \tag{29}$$

This specialized relation is very useful in combining minimum functions resulting from the decomposition of the Patterson synthesis by symmetrically equivalent atoms, and can always be used where symmetry other than an inversion exists in the crystal being analyzed. The relation is extensively used in the discussion which follows.

The practical application of the minimum function

In practice, it is most convenient to start transforming the Patterson synthesis to the approximate electron-density map by first establishing a line image and then using the minimum function to find the images of this line. In the general case, the line image decomposes the Patterson synthesis into two displaced, enantiomorphous solutions. If the crystal (or its projection) is centrosymmetrical, these solutions are, of course, identical. They coincide provided that the line image is established by an 'interaction' between two centrosymmetrically situated atoms. The proper selection of a centrosymmetrical 'interaction' can be guided by (*a*) the relation of rotation peaks to reflection satellites in a Patterson projection, (*b*) by the relation between the peaks on the Patterson projection to those on a parallel Harker projection, or (*c*) by calibration of peaks in terms of the origin peak, as discussed in an earlier section.

Suppose that a two-dimensional Patterson synthesis is to be decomposed by means of the minimum function. Let the centrosymmetrical image point chosen have co-ordinates uv. Then the minimum values of the function

$${}^{uv}M_2(xy)=M\{P(xy);\; P(u+x,\, v+y)\} \tag{30}$$

can be readily determined by examining the numerical values of the Patterson function at all pairs of points xy and $u+x$, $v+y$, and noting the minimum value for each such pair. In order to have the origin of x and y in the resulting approximate electron-density map coincide with an inversion center, Fig. 10 (*a*) and (*b*) shows that this minimum value should be recorded on the map of the minimum function at $\frac{1}{2}u+x$, $\frac{1}{2}v+y$, instead of at xy. This new map contains a set of discrete sampled values of the minimum function ${}^{uv}M_2(xy)$. This analytical method of forming the minimum function has the disadvantage of discontinuity, i.e. a discontinuous sampling of the minimum function is derived from a discontinuous sampling of the Patterson function. If the original point image at uv in the Patterson synthesis does not lie exactly on a sampled value, one must either approximate it by choosing an image point on the nearest sampled value, or resort to a very tedious double interpolation in finding every resulting sample of the minimum function.

A continuous procedure of finding M_2 requires a contoured Patterson map. A line whose ends are at 00 and uv is first established as before and then moved parallel with itself over the entire surface of the Patterson map. One then records at positions corresponding to the midpoint of the line (but on a separate sheet) the minimum value of the Patterson function found at the two ends of the line. Of course, continuous recording is an impractical procedure. The general method can be rendered practical by recording the value of any contour encountered by either end of the line, provided that the encountered contour is the minimum of the two values at the ends of the line. A simplifying procedure is to move the line parallel to itself with one end continuously on the contour of minimum value until the other end of the line crosses a contour of equal value, after which that end controls for awhile.

The theory behind this last method can be put into practical use by a scheme which amounts to pulling the two ends of the line together and examining the points at the two ends at the same time. To do this, one prepares two Patterson syntheses, contoured preferably in color. The two Patterson tracings are placed one over the other so that any xy on one sheet and the corresponding $u+x$, $v+y$ on the other appear together at a common point. As indicated above, this common point is preferably the middle of the line, namely, $\frac{1}{2}u+x$, $\frac{1}{2}v+y$. The minimum value at the continuum of all points of the pair of sheets is now the value of the minimum function ${}^{uv}M_2(x,y)$.

As a practical procedure, the minimum function can be quickly contoured by tracing on a third sheet those contours from the two underlying Patterson maps which represent the smaller values at all points. This is equivalent to drawing that contour of a particular value from one of the two Patterson maps which is nearest a peak in the minimum function. That this procedure is correct can be appreciated by reference to Fig. 11. The diagram shows two peaks, one from each Patterson map, whose heights are shown in the third dimension. The horizontal plane is a contour level L at a particular value of the Patterson function. One observes that, at point a, the right peak has the minimum value, the left peak having a higher value. The contour of the minimum function in the neighborhood of H is therefore the Patterson contour a of value L nearest the highest value of the minimum function H, and not the value e, which is farthest from H. Similarly, b and not f is the contour outlining the other side of the minimum function peak H.

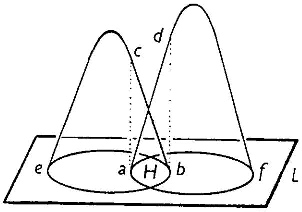

Fig. 11.

By inverting Fig. 11 it can be demonstrated that the minimum function can also be contoured by following that contour of the two Patterson maps which is farthest from each trough in the minimum function. The area within the lowest contour outlining troughs on one Patterson map (shaded in the middle diagram of Fig. 14) has the very interesting property of cancelling peaks on the other Patterson map which are not to become peaks of the electron-density map. In this way the minimum function reduces the n^2 Patterson peaks to the required n peaks of the electron-density map. In a similar way, all contour levels of one Patterson map modulate the features of the other Patterson map which have a higher level.

As a matter of practical procedure it is well to limit the number of contour levels represented on the Patterson map to a few, say 4–7 levels. This spread should be sufficient to represent the electron-density spread of the atoms in the crystal, of course. Furthermore, the routine contouring of the minimum function is much simplified if the two Patterson maps each comprise an area of $1\frac{1}{2}$ cells, specifically 1 translation wide and $1\frac{1}{2}$ translations long. One map should be drawn with the origin in the corner of a cell, the other with the origin in the center of the cell. When forming an M_2 map based upon an inversion image, the origin of the M_2 map occurs half-way between the origins of the two displaced Patterson maps. The selection of the area of $1\frac{1}{2}$ Patterson cells, recommended above, assures that a full non-centrosymmetrical pattern unit of the electron-density cell is obtained from a single setting of the Patterson maps.

The procedure just outlined for mapping the minimum function can be readily generalized. If one wished to derive a contoured map of the minimum function M_p, it could be done by displacing p transparent copies of the Patterson map (with contour levels scaled, if necessary, as indicated below) so that the origins of the several maps come to lie at the coordinates (with respect to the first map) of

$$00,\quad u_1v_1,\quad u_2v_2,\quad \ldots,\quad u_{p-1}v_{p-1}.$$

On a separate transparent sheet the minimum contour of the p maps is then traced according to the procedures outlined above for contouring M_2. If such a single-step method of forming the minimum function map M_p is utilized, the scaling of the contour levels must be in accordance with the coefficients C of (28).

A more convenient way of deriving maps of the minimum functions of higher rank is by way of a stepwise procedure. A formal treatment of the theory was given in the last section in discussing combinatorial properties. The practical procedure is to form two M_2 maps, based upon two different centrosymmetrical image points, and then combine these by contouring the minimum of the two maps to form an M_4 map. When this is done, the correct value of $1/(2\rho)$ in (26) should be recognized by scaling the contours of the two maps appropriately. When the two M_2 maps to be combined are derived from the use of two different Patterson peaks, each caused by the 'interactions' of the same kinds of atoms, then the whole procedure simplifies in that the M_2 maps are directly combined without any scaling of their contours being required.

An important example of this is encountered with every crystal having more symmetry than mere centrosymmetry. For example, in any of the two-dimensional space groups isomorphous with plane point group $2mm$ (for example, $p2mm$, Fig. 12 (a)), the Patterson synthesis has a set of four rotation peaks and four reflection peaks (Fig. 12 (b)). One relation between these four is the trivial relation of centrosymmetry common to all Patterson syntheses. But rotation points not related by centro-symmetry in the Patterson correspond to two different 'interactions' between different pairs of rotation-equivalent atoms of the equivalent set. When one forms an M_2 map based upon one image, say that at uv, this map is, in general, different from the M_2 based upon the image at $\bar{u}v$, although related by symmetry to it. These two maps may be designated ${}^{uv}M_2(xy)$ and ${}^{\bar{u}v}M_2(xy)$ respectively. They can be combined to give a map of a minimum function of greater rank, namely, ${}^{uv,\,\bar{u}v}M_4(xy)$. To do this, one superposes the maps, and traces the minimum of the two. In this example, the two M_2 maps are formed by images based upon atoms $\bar{a}_1a_1$ and $\bar{a}_2a_2$ in Fig. 12 (a). These are related by a horizontal symmetry line. Accordingly, two ${}^{uv}M_2(xy)$ maps are prepared, one is rotated about this horizontal line, placed so that its edges coincide with the other ${}^{uv}M_2(xy)$, and the minimum of the two maps is then contoured. This whole operation is equivalent to using a single image-seeking function which seeks images of the quadrilateral $a_1a_2\bar{a}_1\bar{a}_2$ in Fig. 12 (*a*), whose apices are uv, $u0$, 00 and $0v$ in Fig. 12 (*b*). The whole procedure could therefore also have been done in one step by taking tracings of the four Patterson maps $P(xy)$, displacing them so that they had origins at $uv, u0, 00$, and $0v$ and then tracing the minimum contours from all four at once, as indicated in an earlier discussion. As a matter of practical procedure, tracing the minimum from more than two Patterson maps is not very easy.

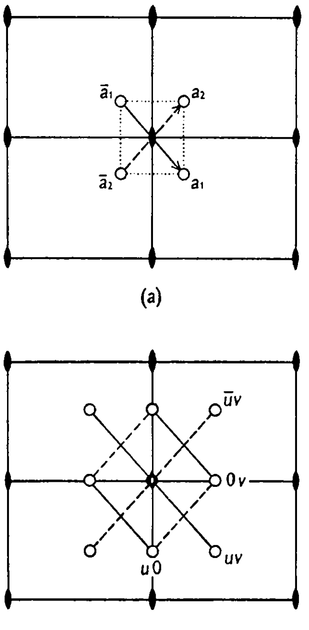

(a)

(*b*)

Fig. 12.

In a similar way, two M_2 maps can be combined directly, provided that they are based upon any two equal Patterson 'interactions'. These need not represent 'interactions' between pairs of atoms related by symmetry. In this procedure all four atoms of the fundamental set are, however, of the same species. The increased rank p of the minimum function M_4, so found, provides a new map which is closer to the electron density than either of the original M_2 maps.

Examples of the use of the minimum function

(1) *Derivation of an approximate* $\rho(xy)$ *from* $P(xy)$ *for berthierite,* $FeSb_2S_4$

The crystal structure of the mineral berthierite, $FeSb_2S_4$, offers a favorable vehicle for demonstrating the use of the minimum function in crystal-structure analysis. The three kinds of atoms in the structure, namely, Sb, Fe and S, contains 51, 26 and 16 electrons respectively, so that electron densities roughly in the ratio 4 : 2 : 1 can be expected in the final electron-density map. Thus the ability of the function to approximate a considerable spread of electron density can be tested. Furthermore, this crystal has moderately large a and b translations, but a small c dimension. This feature permits testing a moderately large electron-density projection area without the usual complication due to overlap of atoms as seen projected through a thick slab of crystal structure. In other words, the (001) projection of this crystal offers an approach to a section through the three-dimensional electron-density function.

Berthierite is orthorhombic (Buerger, 1936), space group *Pnam*, and has four units of $FeSb_2S_4$ in a cell of dimensions

$$a = 11{\cdot}44, \quad b = 14{\cdot}12, \quad c = 3{\cdot}76\ \text{A}.$$

The space group *Pnam* projects on (001) as the two-dimensional space group *p*2*gg*. The symmetry elements of this group are shown in Fig. 13 (*a*).

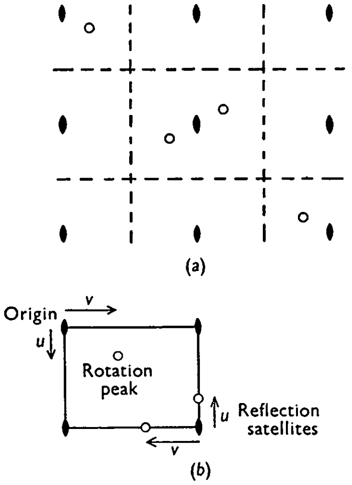

(a)

(*b*)

Fig. 13.

Data for the intensities of *hk*0 were obtained from a single precession photograph. The photograph was processed by the M.I.T. modification of the Dawton method, from which integrated intensities were determined. After correcting for Lorentz and polarization factors, a Patterson projection $P(xy)$ was computed. The representative quarter cell of this is shown in the upper middle part of Fig. 14.

This Patterson was not interpretable by any standard methods, and even the location of the heaviest atoms could not be fixed with certainty with its aid. The relation between the co-ordinates of any inversion peak and the glide-reflection satellites in a quarter cell of $P(xy)$ for this symmetry is shown in Fig. 13 (*b*). A start on the solution can be made by noting that the quarter cell contains two antimony atoms, and that there are two sets of reflection satellites. These determine four possible locations of rotation peaks, according to the relations shown in Fig. 13 (*b*). Two such locations, marked by crosses in $P(xy)$ in the upper middle of Fig. 14, are near more or less acceptable peaks, although not actually on their maximum positions. The best location is the lower left cross. If this peak and the two corresponding satellites are truly a set of 'interactions' within a symmetrically related set of atoms, the two reflection satellite peaks should have weight 2, while the rotation peak should have unit weight, a relation which is not obeyed. Such lack of harmony in the weighting of sets of symmetrically related 'interactions' is commonly observed and may, perhaps, be attributed to differences in the relative thermal motions of atoms related by different symmetries.

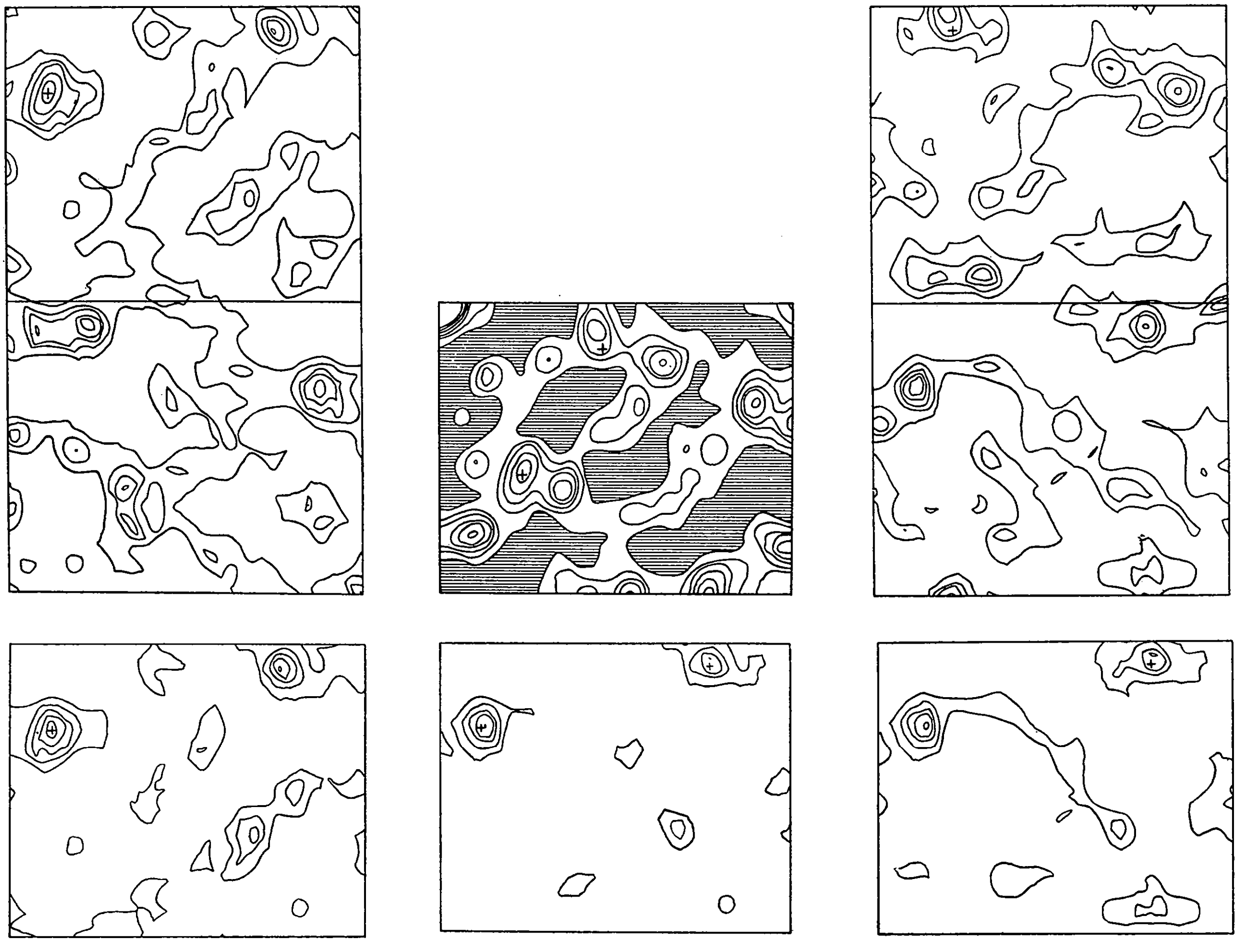

Fig. 14.

Accepting the lower left cross provisionally as the correct location of a rotation (i.e. a centrosymmetrical) 'interaction', one can then set up the minimum function based upon the co-ordinates of this point plus those of the origin, namely, ${}^{0\cdot297,\ 0\cdot118}M_2(xy)$. The minimum function is then simply found by placing one transparent Patterson map over another, the origin of one being placed at the cross of the other. By contouring the minimum, as described in the last section, the large M_2 map is derived which is shown in the upper left of Fig. 14. Now, a glide line runs vertically through the center of this map, as shown in Fig. 13 (*a*). Consequently the lower quarter cell should be the glide equivalent of the upper quarter cell. These two quarter cells can therefore be combined to form a map of an M_4 function. To do this, the lower quarter cell is traced, laid directly over the upper quarter cell in reversed position (the glide operation), and the minimum contour of the two quarters traced. This results in the M_4 map shown below it in Fig. 14. Such a combination can always be made in crystals having greater symmetry than merely an inversion.

Some of the major features of the distribution of atoms in the cell are already plain in this M_4 map. The original Patterson peak at the lower left cross has given rise to a heavy atom at about 0·147, 0·060, and also another large peak of about equal magnitude at about 0·040, 0·384. The last is obviously to be interpreted as the other antimony atom of the quarter cell. Its location is consistent with the upper right cross of $P(xy)$ in Fig. 14. Using this cross as an image point, another M_2 can be graphically derived, namely, ${}^{0\cdot080,\ 0\cdot233}M_2(xy)$. This is shown in the upper right of

Fig. 14. The upper and lower halves of this are combined to form an M_4 map, as in the last case. The result is shown just below ${}^{0\cdot080,\,0\cdot233}M_2(xy)$.

Finally, the two M_4's can be combined to provide an M_8, specifically ${}^{0\cdot297,\,0\cdot118;\;0\cdot080,\,0\cdot233}M_8(xy)$. This is shown at the middle bottom of Fig. 14. This function is a sufficiently close approximation to the electron density so that all the atoms of the crystal structure can now be identified. The map of M_8 shows two large peaks of relative weight 4, one peak of relative weight 2, and four peaks of relative weight 1. These are obviously to be identified with 2 Sb, 1 Fe and 4 S, respectively. That this is at least approximately the correct structure can be demonstrated by comparing the original precession photograph with the fly's-eye photograph based upon the atom locations and identifications given by M_8.

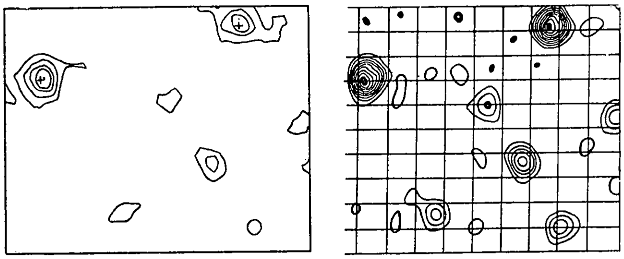
(a) (b)

Fig. 15. Comparison of the map of the minimum function $M_8(xy)$ with the map of $\rho(xy)$ for berthierite. The latter, shown at the right, was prepared by using the measured $|F|$'s together with phases based upon the atom location of $M_8(xy)$. The Fourier synthesis is a photograph of the synthesis produced by the Pennsylvania State College X-RAC, by courtesy of Prof. Ray Pepinsky.

(2) *Derivation of an approximate* $\rho(xy)$ *from* $P(xy)$ *for claudetite,* As_2O_3

The space group of the mineral claudetite, As_2O_3, is $P2_1/n$, and its cell dimensions are

$$a=5\cdot26,\quad b=12\cdot87,\quad c=4\cdot54\text{ A.},\quad \beta=93°\,49'.$$

This cell contains $4As_2O_3$. Space group $P2_1/n$ projects on (001) as the two-dimensional space group $p2gg$. The symmetry of the projection and its Patterson are the same as those shown in Fig. 13.

Dr Alfred E. Frueh is investigating the structure of claudetite and has kindly supplied me with numerical values of the Patterson projection $P(xy)$, shown in Fig. 16(*a*). I have deduced an approximate electron density for this projection by minimum-function methods. The start was an acceptance of the location, marked on $P(xy)$ by a cross, as a rotation peak substantiated by reflection satellites. This was the only set of features of the Patterson projection which was subject to interpretation. The solution followed steps described in detail under the discussion of berthierite. The end-result is a map of the minimum function $M_8(xy)$ shown in Fig. 16(*b*).

Dr Frueh has derived the electron-density projection, $\rho(xy)$, by methods not involving image-seeking functions. His map, which he has kindly allowed me to reproduce, is shown in Fig. 16(*c*). No attempt is made here to discuss the locations of atoms in the map; attention is merely called to the general agreement of the topography of $M_8(xy)$ and $\rho(xy)$.

In Fig. 16(*d*) there is presented for comparison a map of the product function $\sqrt{\Pi_2(xy)}$ for claudetite. This

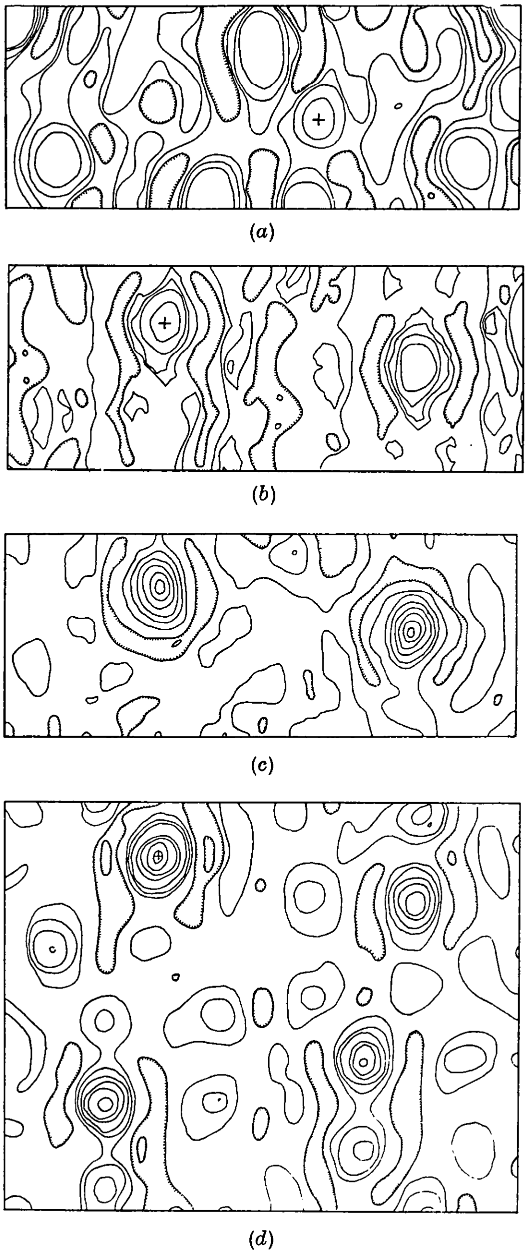
(a)
(b)
(c)
(d)

Fig. 16. Image-seeking functions applied to the interpretation of the Patterson projection of claudetite, monoclinic As_2O_3. The symmetry relations are the same as shown in Fig. 13. (*a*) Quarter cell of $P(xy)$, prepared from numerical data supplied by Dr Alfred E. Frueh. (*b*) Map of the minimum function, $M_8(xy)$. (*c*) Electron-density map, $\rho(xy)$, as found by Dr Alfred E. Frueh by methods not based upon the use of image-seeking functions. (Used by permission of Dr Alfred E. Frueh.) (*d*) Map of the product function, $\sqrt{\Pi_2(xy)}$, based upon the location marked by the cross in $P(xy)$.

map is based only on a line image generated by connecting the location of the cross marked in $P(xy)$ with the origin. The resemblance of this product-function map with the electron-density map is reasonably good, especially when it is realized that it is only a Π_2 map.

Remarks on other current methods of interpreting Patterson maps

Since the writer demonstrated that vector sets can be interpreted, a number of supposedly different rival methods have arisen which have also been proposed as devices for solving Patterson maps (Clastre & Gay, 1950*a*, *b*, *c*; Garrido, 1950*a*; Robertson, 1951; McLachlan, 1951). Most of these have a common feature; they deal with Patterson peaks as if they were points on a vector set consisting of discrete points. These peaks are treated by a geometrical device (usually a translation) which is merely another description for finding images. Such methods are therefore not different, in essence, from those first described in VS, except that a different language is used in the discussion (Mauguin, 1950). They are accordingly no more powerful than vector-set methods used for discrete points. To use them for interpreting Patterson maps, the Patterson peaks must, in essence, be regarded as a map of weighted points. These methods are not useful as they stand in interpreting a typical Patterson synthesis because, as pointed out earlier in this paper, the high values of a typical Patterson synthesis are often not single peaks. In fact, they usually arise owing to a coalescence of many peaks. To treat such a composite feature as analogous to a point on a vector set of discrete points is most misleading.

The 'vector convergence method' (Beevers & Robertson, 1950; Robertson, 1951) can be discussed along more quantitative lines. In its best form it appears to be equivalent to using a sum function as an image-seeking function. In other words, as the image-seeking polygon roves the Patterson synthesis, the sum of the Patterson values at its several vertices is continuously laid down. If this function is studied with respect to a line image, as in Fig. 8, it will be seen that every time the roving line encounters a point of the vector set at either of its ends, it lays down a point of weight either a or b. There are therefore $2n^2$ solution points laid down, of which n (plus $n-2$ more for line images only) coincide and have weight $(a+b)$. Clearly, *even with a vector set of discrete points*, the vector convergence method provides a much more remote approximation to the electron density than either the product function or the minimum function, which, in this simple case give an *exact* solution for the electron density.

References

Beevers, C. A. & Robertson, J. H. (1950). *Acta Cryst.* **3**, 164.

Buerger, M. J. (1936). *Amer. Min.* **21**, 442.

Buerger, M. J. (1946). *J. Appl. Phys.* **17**, 479.

Buerger, M. J. (1948*a*). *Phys. Rev.* **73**, 927.

Buerger, M. J. (1948*b*). *Proc. Nat. Acad. Sci., Wash.*, **34**, 277.

Buerger, M. J. (1950*a*). *Acta Cryst.* **3**, 87.

Buerger, M. J. (1950*b*). 'The Application of Image Theory to Crystal Structure Analysis'. Paper presented 6 April 1950 at the Phase and Computor Symposium, Pennsylvania State College.

Buerger, M. J. (1950*c*). *Proc. Nat. Acad. Sci., Wash.*, **36**, 329, footnote 13.

Buerger, M. J. (1950*d*). *Proc. Nat. Acad. Sci., Wash.*, **36**, 376.

Buerger, M. J. (1950*e*). *Proc. Nat. Acad. Sci., Wash.*, **36**, 738.

Clastre, J. & Gay, R. (1950*a*). *C.R. Acad. Sci., Paris*, **230**, 1976.

Clastre, J. & Gay, R. (1950*b*). *Bull. Soc. franç. Minér.* **73**, 202.

Clastre, J. & Gay, R. (1950*c*). *J. Phys. Radium*, **11**, 75.

Garrido, J. (1950*a*). *C.R. Acad. Sci., Paris*, **230**, 1878.

Garrido, J. (1950*b*). *C.R. Acad. Sci., Paris*, **231**, 297.

Mauguin, C. (1950). *C.R. Acad. Sci., Paris*, **230**, 1879.

McLachlan, D., Jr. (1951). *Proc. Nat. Acad. Sci., Wash.*, **37**, 115.

Patterson, A. L. (1934). *Phys. Rev.* **46**, 372.

Patterson, A. L. (1935). *Z. Krystallogr.* **90**, 517.

Robertson, J. H. (1951). *Acta Cryst.* **4**, 63.

Wrinch, D. (1939). *Phil. Mag.* **27**, 98.